AiMT Advances in Military Technology
Vol. 9, No. 2, December 2014

Investigation of Airflow in Internal Recirculation Channel of Centrifugal Compressor

M. Poledno*, P. Kmoch and A. Jílek

Department of Airspace and Rocket Technologies, University of Defence, Brno, Czech Republic

The manuscript was received on 16 April 2014 and was accepted after revision for publication on 27 November 2014.

Abstract:

Contemporary high pressure ratio centrifugal compressors have a narrow stable operating. In order to achieve a wider stable operating region, some anti-surge measures can be used, such as an internal recirculation channel (IRC). This article presents a study of the airflow in IRC of a centrifugal compressor. A model of such channel was designed and manufactured in order to investigate the influence of various IRC inlet slot geometry on air flow parameters. Numerical simulation of the airflow for selected variants was also performed. Results of the simulation together with results of the experiment enable us to analyse the airflow in the area of the inlet slot and to find out its most suitable geometry.

Keywords:

Centrifugal compressor, internal bleed system, internal recirculation channel, stable operating region

1. Introduction

In the aviation, centrifugal compressors find their place in gas turbine engines operating at low air mass flow rate like low-power turboshaft engines, auxiliary power units (APU's) or special turbojet engines. They are also used as turbochargers in aircraft piston engines. Such compressors are simple, light, easy to manufacture and thus fairly inexpensive.

A schematic view of a centrifugal compressor is given in Fig. 1. The compressor consists of an intake duct (0-1), an impeller (1-2), vaneless diffuser (2-3), vaned diffuser (3-4) and an outlet duct (4-5) [1].

* *Corresponding author: Department of Airspace and Rocket Technologies, University of Defence, Kounicova 65, 662 10 Brno, Czech Republic, phone: +420 973 445 143, E-mail: martin.poledno@gmail.com*

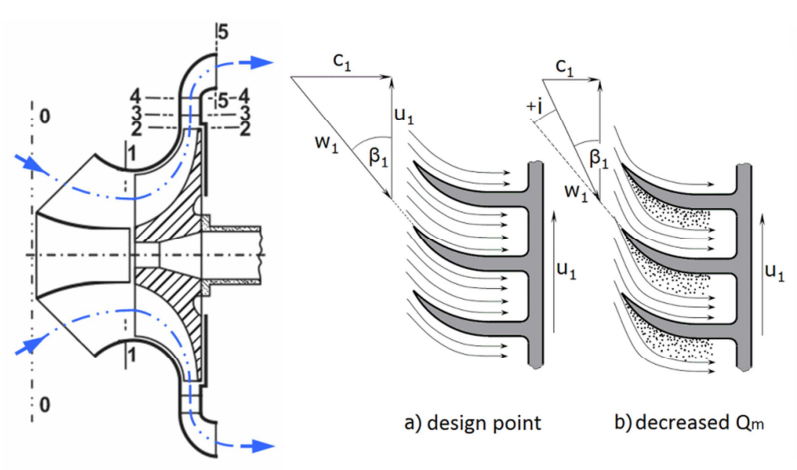

Fig. 1 Scheme of centrifugal compressor [1] and flow separation in impeller

An analysis of the thermodynamic cycle of a gas turbine engine [2] shows that high values of compressor pressure ratio are needed in order to achieve the necessary power of the engine, especially for high temperature in front of the turbine. However, such high pressure ratio compressors have a narrow stable operating region. This region is defined by the difference of the air mass flow rate from the surge line to the aerodynamic choke. Due to the narrow stable operating region, the transient behaviour is negatively affected, which can cause decrease in the operability of such gas turbine engines.

Compressor pressure ratio π_{ct} is defined by the total pressure at the compressor outlet p_{5t} and the total pressure in front of the impeller p_{1t} (see Fig. 1):

$$\pi_{ct} = \frac{p_{5t}}{p_{1t}} \tag{1}$$

Compressor isentropic efficiency η_c is calculated from total temperatures, where T^*_{5t} is an isentropic temperature at the compressor outlet:

$$\eta_c = \frac{T^*_{5t} - T_{1t}}{T_{5t} - T_{1t}} \tag{2}$$

Unstable operating states of the compressor are caused by a rapid drop of the pressure ratio. The compressor pressure ratio drops as the pressure loss rises due to the separation of the flow at the impeller or diffuser vanes.

As the air mass flow rate through the compressor Q_m changes, the absolute velocity of the airflow in the inlet duct c_1 changes as well. Supposing that the rotor speed is constant (i.e. tangential velocity u_1 at given radius is constant), the incidence angle i of the relative stream w_1 changes with respect to the axial velocity c_1.

At the design point (Fig. 1a), the incidence angle i is close to zero, there is no separation of the airflow in the impeller and the pressure ratio and the efficiency will come up to the highest values for the given rotor speed. In case of decreased air mass flow rate Q_m through the compressor (Fig. 1b) the incidence angle i reaches positive values and the flow begins to separate. At high values of the incidence angle i the separation rapidly spreads along the flow channel, which causes a significant pressure loss and can lead to the unstable operation of a centrifugal compressor [1]. There is a

similar flow separation caused by the change of the incidence angle in the vaned diffuser. This means that the stable operating region of a centrifugal compressor can be extended by appropriate modification of the flow field in front of the impeller in order to achieve lower values of the incidence angle on the impeller vanes.

One of the methods how to extend the stable operating region is to use an internal recirculation channel (IRC) that allows partial recirculation of the compressed air. Using this channel, part of the compressed air flows back from the inducer to the inlet duct, where it influences the flow field in front of the impeller in order to suppress stall at the inducer vanes. Such recirculation channel does not complicate the compressor design, it is easy to manufacture and it can partially improve the compressor characteristics.

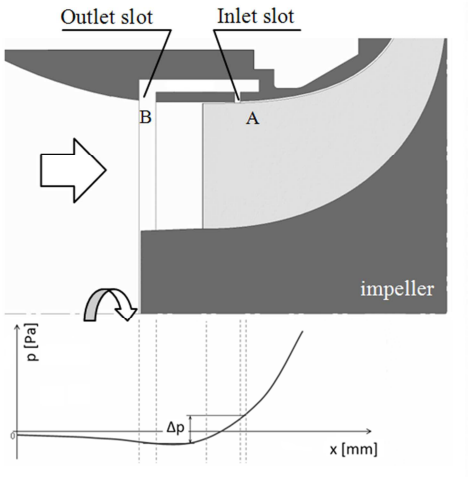

Fig. 2 Scheme of internal recirculation channel

The internal recirculation channel (see Fig. 2) consists of an inlet slot (A) above the impeller, an outlet slot (B) in the inlet duct and an annular channel connecting them. The flow through the IRC is conditioned by static pressure gradient Δp between the inlet slot and the outlet slot. The position of the inlet slot and the outlet slot has significant influence on the pressure gradient Δp, as shown in Fig. 2, where a typical static pressure distribution along the compressor casing is shown. It is important to note that the pressure distribution is generally variable and depends on the actual operating point of the compressor. Internal recirculation channel partially extends the stable operating region of the compressor (see Fig. 3) as it was proved by many experiments.

The use of IRC in a centrifugal compressor with design pressure ratio $\pi_{ct} = 4.2$ [3] caused an extension of the stable operating region (Fig. 3), however a drop of compressor pressure ratio and efficiency occurred at the high rotation speed. Similar results were obtained for turbocharger with a fairly low design pressure ratio $\pi_{ct} = 3.2$ [4]. Six different IRC geometries were investigated in [5]. The results were similar to those described in [3]. Measurements on Cummins turbocharger [6, 7] were carried out for 3 rotation speeds (68 %, 87 % and 100 %). This experiment was focused on the influence of the inlet slot position relative to the inducer leading edge and the inlet slot width on the compressor map. In the following experiment [8, 9] the influence of vanes inside the IRC was investigated. Results of the individual reports mentioned above indicate how the compressor map is affected by the IRC: stable operating region is

enhanced, but usually there is some compressor pressure ratio and efficiency drop, especially at high rotation speed.

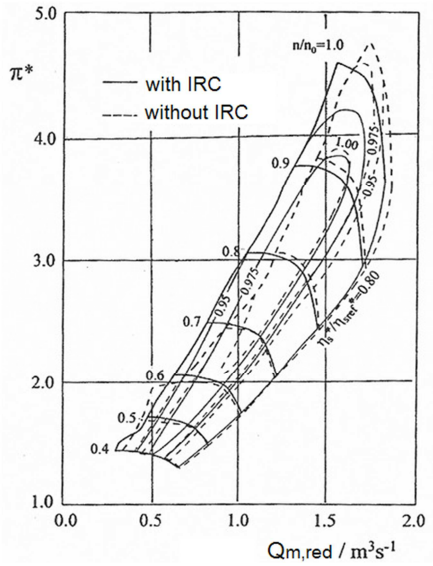

Fig. 3 Compressor map [3]

However, in the available references there is a lack of theoretical basis for IRC design. Often, centrifugal compressor is manufactured with unfounded dimensions and position of the IRC. Such recirculation channel designs are verified only by an experiment on a real compressor, which makes it impossible to pay detailed attention to the airflow in the recirculation channel itself. An influence of the outlet slot geometry on the flow field in front of the impeller was investigated both experimentally and by simulation in [10]. The above mentioned research works do not concern the influence of the IRC inlet slot geometry on the energy losses of the airflow through the IRC.

2. Physical Model of Internal Recirculation Channel

In order to investigate the airflow in the IRC of a centrifugal compressor, a physical model of one was designed and manufactured as a part of a research work at the University of Defence [11].

A concept of the model is shown in Fig. 4. The model can be divided into three main areas: the IRC itself (A-B), the main duct (D-E), which corresponds to the inlet duct of a centrifugal compressor, and the annular supply duct (C-F), which the compressed air is delivered through.

Compressed air from an external supply Q_1 is delivered to the model using nine inlet pipes attached to the threaded holes (C) in the rear cover. The holes in the cover are skewed to the axis of the model in order to give the air the highest possible swirl, which is present on real centrifugal compressors. The airflow Q_1 runs through the annular supply duct to the place of the inlet slot (A), where it is divided into two streams: Q_2 which enters the recirculation channel and Q_3 which reverses its direction and flows out into the atmosphere (F).

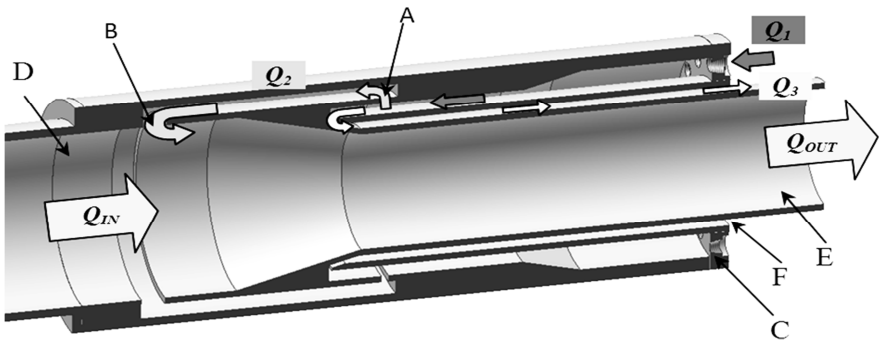

Fig. 4 Concept of IRC model

This approach should imitate the airflow along the casing wall of a real centrifugal compressor in place of its inlet slot, where the air flows through the impeller and only its small amount (most likely from the near-wall areas) enters the recirculation channel. The airflow Q_2 exits the recirculation channel through the outlet slot (B) and mixes up with the airflow Q_{IN} in the main duct. Therefore, the air mass flow rate through the internal recirculation channel Q_2 can be determined by the difference between the air mass flow rate Q_{OUT} at the model outflow and Q_{IN} at the model inlet.

Based on the previous concept, the IRC model was designed and manufactured. The model is shown in Fig. 5 and consists of outer casing (1), front cover (2), rear cover with skewed air supply tubes (3), inner part (4), central tube (5), exchangeable rings ”A” (6), ”B” (7), ”C” (8) and ”D” (9), front pipe flange (10), front pipe (11) and output pipe (12). The inlet slot of IRC is formed by exchangeable rings ”C” and ”D”, while the outlet slot is formed by rings ”A” and ”B”. These rings can be removed, adjusted and mounted again. This allows us to modify the geometry of the input and output slots quite easily without making any irreversible changes on the IRC model.

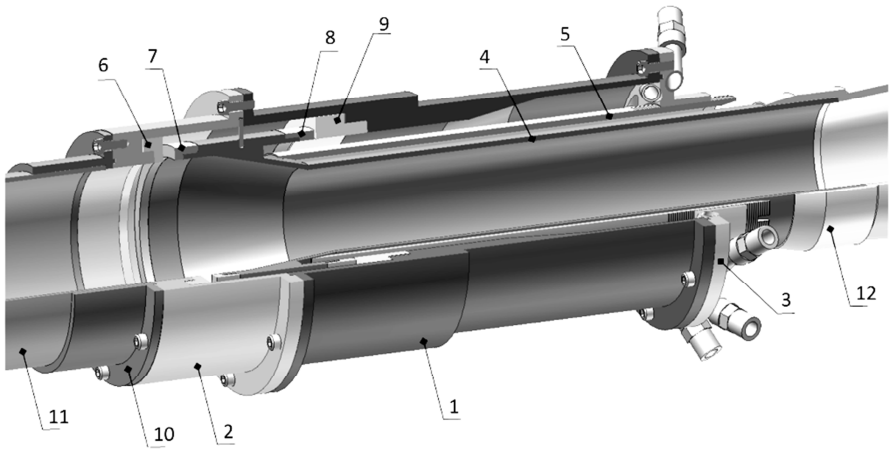

Fig. 5 Design of IRC model

Figure 6 shows locations of pressure probes and taps installed on the IRC model. The temperature of air entering the model is measured by thermocouple. In section ”1” - in front of the inlet slot formed by ”C” and ”D” rings - there is a 3-hole yaw probe allowing us to measure total and static pressure as well as the velocity angle of the swirled flow. In the same section there are four wall pressure taps uniformly distributed along the circumference, which enables us to measure the static pressure in this section. At the end of the recirculation channel there are static pressure taps and a 3-hole cylindrical probe, which is due to its size situated few millimetres further - inside the outlet slot. Static pressure taps in section ”4” are located in the main duct in front of the IRC outlet slot.

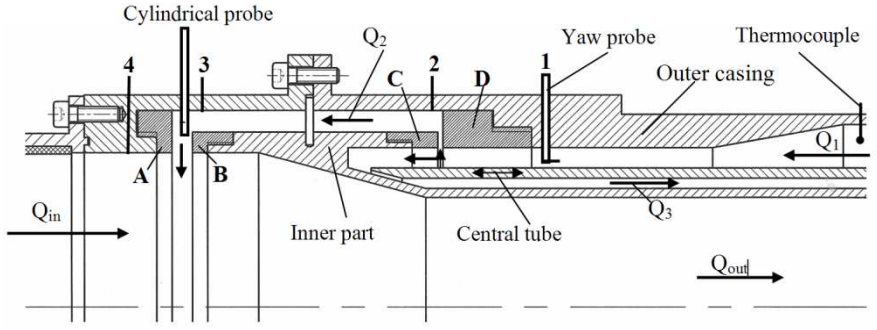

Fig. 6 Scheme of IRC model with pressure probes and taps location

3. Experiment

Series of measurements were carried out on the IRC model to determine the dependency of the air mass flow rate through the IRC channel and energy losses of the airflow for various pressure gradients and for various geometrical configurations of the inlet slot. The air mass flow rate through the recirculation channel Q_2 is determined by the difference of mass flow rate Q_{OUT} and Q_{IN} measured by two orifices (see Chapter 3.1). Pressure gradient on the recirculation channel Δp_{14} is defined by the difference of static pressure in front of the inlet slot p_1 and static pressure in front of the outlet slot p_4. Energy losses of the airflow in the recirculation channel are evaluated by total pressure conservation coefficient $\sigma_{IRC} = p_{3t} / p_{1t}$ and plotted against the Mach number M_1. The Mach number is evaluated using the total and static pressures measured in section ”1”. Geometrical configuration of the inlet slot can be varied by adjusting the exchangeable rings ”C” and ”D”.

3.1 Description of Experimental Stand

The experimental stand is shown in Fig. 7. The IRC model (1) is on its both sides attached to orifices (2, 3) using plastic pipes (5). The orifices are used to measure the air mass flow rate entering the model (Q_{IN}) and exiting the model (Q_{OUT}). The measurements were performed in accordance with standards [12]. The system is connected to the inlet of the industrial fan (7) using a flexible tube (6). A neck (4) prevents from separation of the airflow on a sharp edge of the pipe. Compressed air (Q_1) is delivered to the IRC model from a pressure vessel. More detailed description of the experiment and the data acquisition system is given in [11].

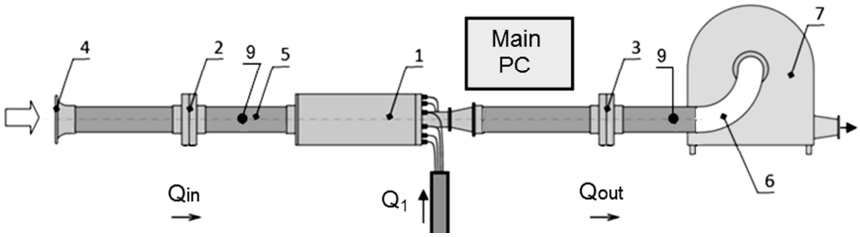

Fig. 7 Scheme of experimental stand

3.2 Inlet Slot Configuration

Combining different values of the inlet slot width, the inlet slot leading edge modification and the depth of the cavity (see Fig. 8), seven variants of the IRC inlet slot were considered:

- angle 90°, width 2 mm, sharp leading edge (90-2SE)
- angle 90°, width 2 mm, bevel leading edge (90-BE)
- angle 90°, width 2.5 mm, bevel leading edge (90-2.5BE)
- angle 60°, width 2 mm (60-2)
- angle 60°, width 2.5 mm (60-2.5)
- angle 45°, width 2 mm (45-2)
- angle 45°, width 2.5 mm (45-2.5)

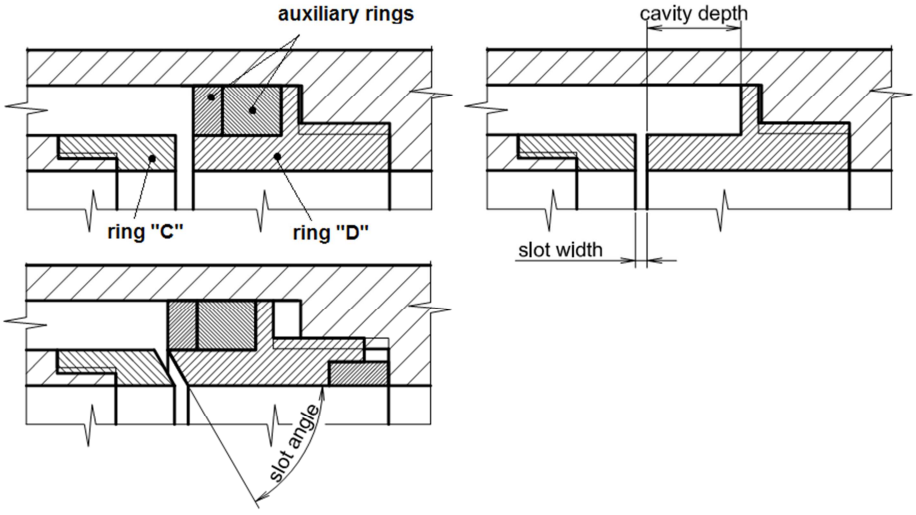

Fig. 8 IRC geometry configuration

Moreover, each of these variants was measured with variable cavity depth. The cavity depth was adjusted by inserting the auxiliary rings of 5 mm and 10 mm width (see Fig. 8). In this way, the cavity depth could be altered to 0 mm (C0), 5 mm (C5), 10 mm (C10) or 15 mm (C15).

3.3 Results of the Experiment

First series of measurements were carried out for 90° inlet slot angle variants. The resulting diagrams in Fig. 9 and Fig. 10 show that the variant with 2 mm slot width and sharp leading edge (90-2SE) gives the poorest results in terms of the lowest air mass flow rate Q_2 trough the IRC at given pressure gradients Δp_{14} and the highest energy losses at given M_1.

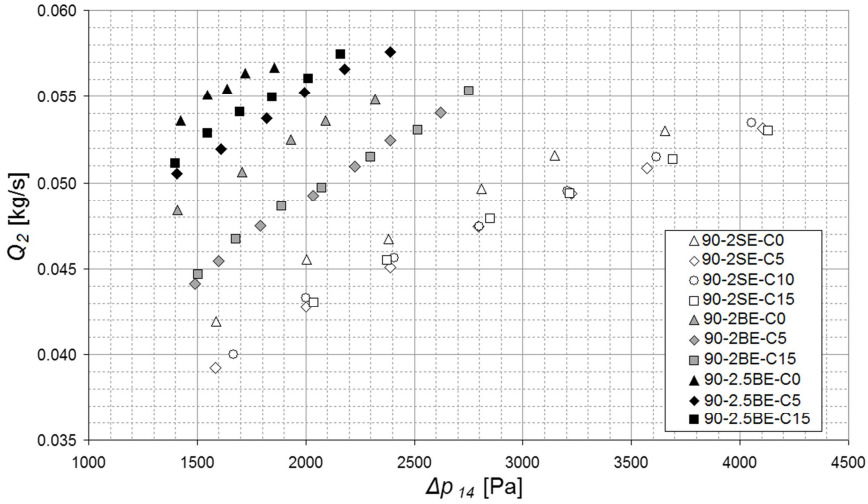

Fig. 9 Measurement results of variants with 90° inlet slot angle, IRC air mass flow rate vs. pressure gradient

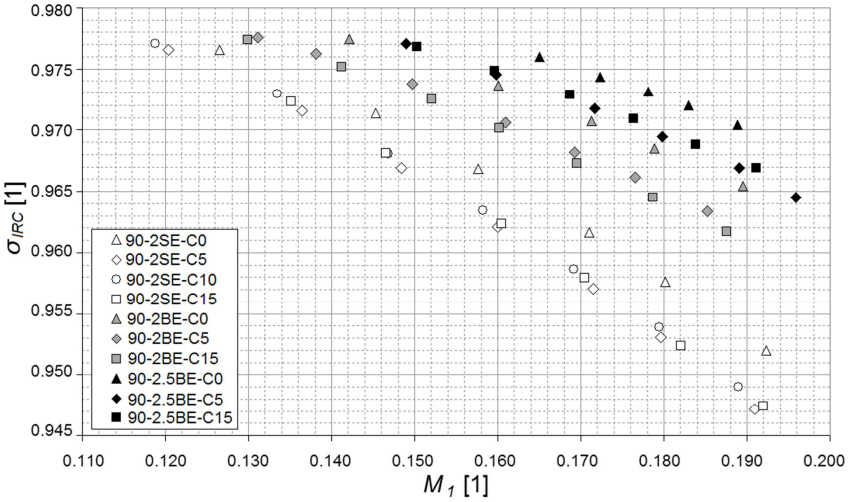

Fig. 10 Measurement results of variants with 90° inlet slot angle, pressure losses vs. inlet Mach number

Effect of variable cavity depth was also discovered. The C0 variant (without any cavity, i.e. with both auxiliary rings installed) showed better results than all the other variants. The remaining three cavity depths variants (C5, C10 and C15) gave slightly worse results than C0. Moreover, variants C10 and C15 showed almost identical results. In terms of this fact, the C10 variant was excluded from all the following measurements.

The results of variant 90-2BE with bevel leading edges of the inlet slot showed that even a slight modification of the slot leading edge can increase the Q_2 at given Δp_{14} and decrease the energy losses of the flow (see Fig. 9 and Fig. 10). For the inlet slot width of 2.5 mm, the results are even better. The impact of various cavity depths is the same as described above for all 90° variants (90-2SE, 90-2BE and 90-2.5BE).

Next, variants with skewed inlet slot (angles 60° and 45°) were tested. In this article, only the results of 45° variant are presented, as the differences between 45° and 60° variants were found fairly insignificant [11].

The measurements were carried out for 2 mm and 2.5 mm inlet slot width (45-2 and 45-2.5) and for different cavity depth C0, C5 and C15 (see Fig. 11 and Fig. 12). It is obvious that an increase of the inlet slot width from 2 mm to 2.5 mm causes a higher IRC air mass flow rate at given pressure gradient and lower pressure losses. In case of the 2 mm inlet slot width, the variant without the cavity (C0) gives slightly worse results than C5 and C15, which is the opposite to previous measurements with 90° inlet slot angle. The difference between results of particular cavity depths gets less noticeable as the inlet slot width is increased. Comparing the results of variants with inlet slot angle 90° and 45°, it is possible to state that the inlet slot angle makes only a little difference.

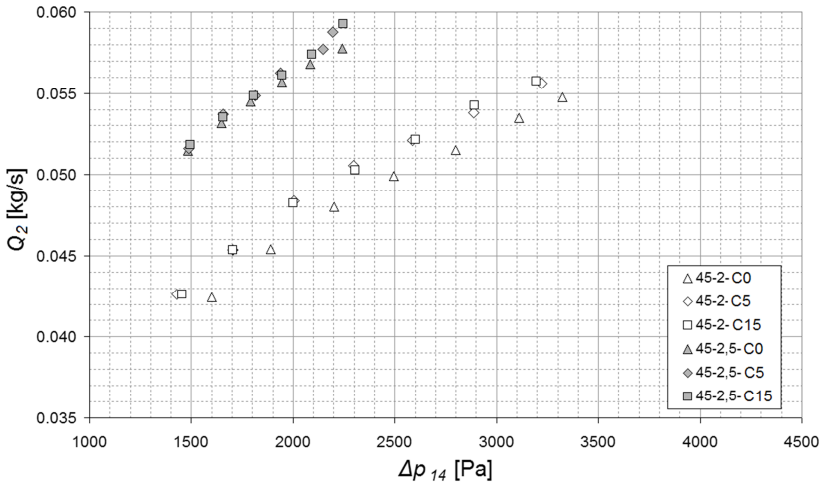

Fig. 11 Measurement results of variants with 45° inlet slot angle, IRC air mass flow rate vs. pressure gradient

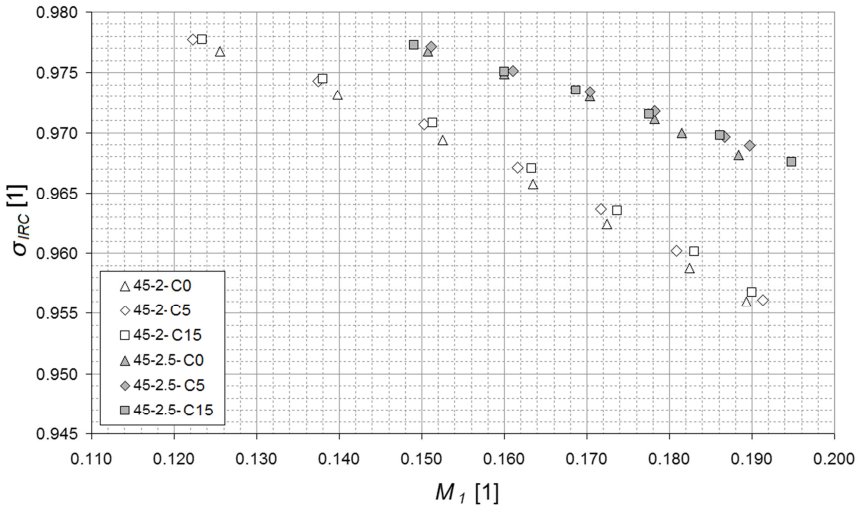

Fig. 12 Measurement results of variants with 45° inlet slot angle, pressure losses vs. inlet Mach number

4. CFD Simulation

The numerical simulation was performed in ANSYS Fluent in order to obtain a detailed picture of the flow field inside the IRC which can enable us to determine the origin of pressure losses for particular IRC geometry variants.

Tab. 1 Summary of simulated variants

90-2SE	90-2BE	60-2	45-2
C0, C5, C10, C15	C0, C5, C15	C0, C5, C15	C0, C5, C15

As the IRC model is axisymmetric and the flow field inside it can be considered axisymmetric too, the simulation was based on this simplifying condition. For the purpose of simulation, only the variants with the 2 mm inlet slot width were chosen (see Tab. 1).

4.1 Simulation Results in General

Numerical simulation was performed for 13 chosen variants of IRC geometry. Each variant was solved for three pressure gradients approximately in the same range as pressure gradients that were reached during the experiment. This allows us to compare the simulation results with the results of the experiment. Following paragraph provides a description of the resultant flow field for one of the simulated variants (90-2SE-C15, Δp_{14} = 3.3 kPa).

Figure 13 shows streamlines which can visualize the flow field character and reveal areas where vortices are present. Attention will be paid mostly to the vortex ”A” which is formed in the IRC cavity and to the flow separation inside the inlet slot ”B”. Air flowing through the inlet slot bends in the direction of its further flow and attaches to the upper wall of the channel. This generates a vast vortex in area ”C” which covers approximately 80 % of channel length. Another vortex is present in area ”D” which is

typical only of narrow supply duct of the IRC model. In area ”E”, where the air exits the IRC and mixes up with the flow in the main duct, another vortex is generated, but this area is not an object of our investigation.

The numerical simulation revealed that the vortex ”C” does not change significantly for particular solutions, that is why a detailed attention was paid mainly to the areas ”A” and ”B”.

The axial component of the velocity increases significantly in the IRC as a result of the reduced effective cross-section due to the vortex in area ”C”. At the end of this area the flow expands to the whole cross-section of the channel and the axial velocity component substantially decreases. The radial component of the flow velocity reaches higher values only in the inlet and the outlet slot of the IRC.

In the supply duct (see Fig. 4) the tangential velocity component is rather high which corresponds to highly swirled flow (swirl angle $\alpha = 75°$ was defined in boundary conditions at the inlet). As the flow enters the IRC inlet slot, the tangential component of the velocity decreases in compliance with the angular momentum conservation law. The decrease of both axial and tangential components of the velocity at the end of the IRC can lead to rather insignificant change of the swirl angle α of the flow. Particular simulated variants vary only by the inlet slot geometry and the cavity depth.

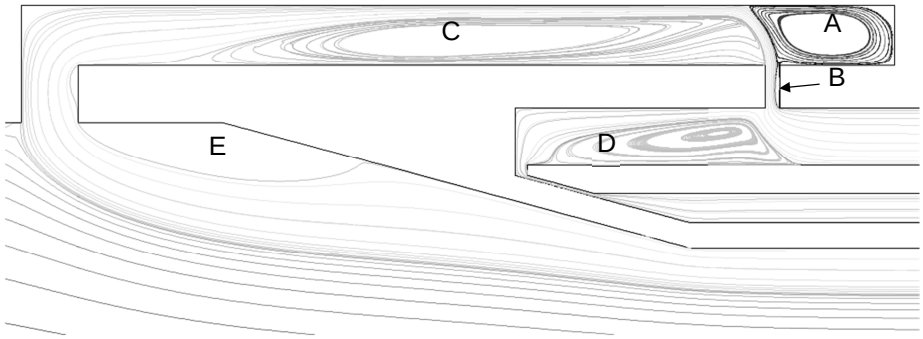

Fig. 13 Streamlines of simulated flow

Attention is primarily paid to the flow field in this region. Simulation results show that the flow field in other IRC regions has approximately the same character in all solved variants.

4.2 Simulation Results of Vertical Inlet Slot Variants

Results of the numerical simulation are presented by a pair of images, where the left one represents the velocity magnitude distribution and the right one represents streamlines in given region. The resultant flow fields of variants 90-2SE-C0 and 90-2SE-C5 are shown in Fig. 14. It is obvious that in the cavity area a vortex is generated. For the C0 variant, without the cavity, a restricted vortex is located in the upper corner of the recirculation channel. On the other hand, in case of the C5 variant, the vortex fills the whole cavity. The vortex intensity (corresponding to the speed of its rotation) is the highest for the C5 variant. In case of the C10 and C15 variants, the vortex fills up the whole area of the cavity too, but its intensity gets lower.

If a link is put between the statements mentioned above and pressure losses, described in the diagram in Fig. 10, it is possible to presume that the vortex in the cavity area causes a pressure loss, as it drains the energy from the airflow exiting the inlet slot. The pressure losses were lower in case of the C0 variant and more significant in case of other cavity depths. This corresponds to the size and intensity of the vortex generated in the cavity area.

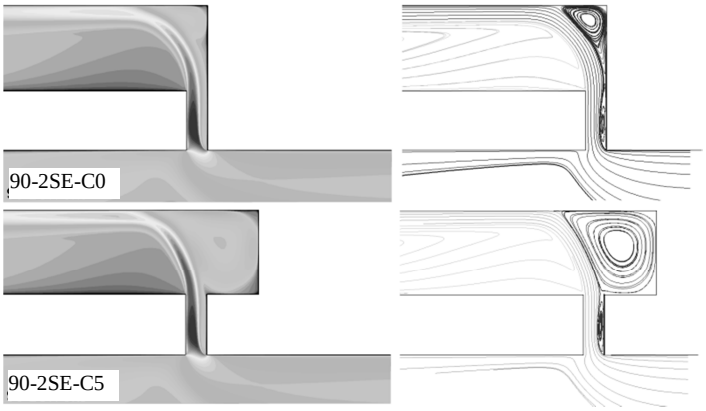

Fig. 14 Flow field in IRC inlet slot, variants 90-2SE

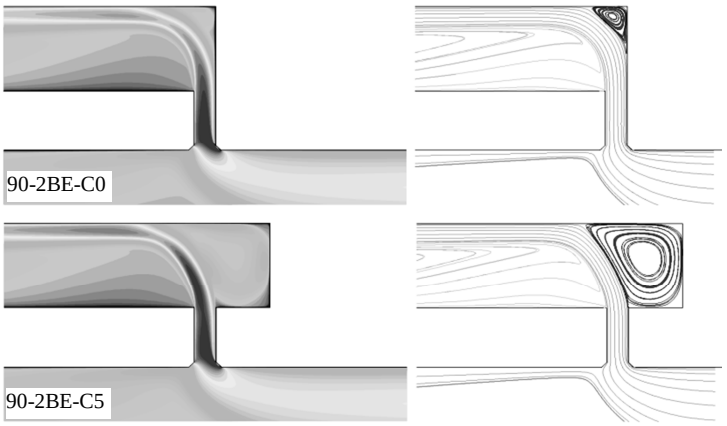

Fig. 15 Flow field in IRC inlet slot, variants 90-2BE

If we compare the sharp edge of the inlet slot (90-2SE, Fig. 14) with the bevel edge (90-2BE, Fig. 15), it is obvious that the sharp edge causes a flow separation in the inlet slot. The effective cross-section area of the inlet slot is significantly reduced (see Fig. 14). On the other hand, in case of the edge bevelled just by $0.5 \times 45°$ there is practically no flow separation.

The influence of the cavity depth is the same as it was mentioned for the previous variant. For the variant 90-2BE-C0, without the cavity, the vortex located in the upper corner of the channel is even smaller than in case of the sharp inlet slot edge (Fig. 15).

4.3 Simulation Results of Skewed Inlet Slot Variants

The numerical simulation was performed also for variants with skewed inlet slot at the angle of 60 and 45 degrees. In this case, the airflow enters the recirculation channel in the direction given by the skewed inlet slot. That means that even in the case of no cavity (C0), in the upper corner of the channel there is enough space for intensive vortex to be generated (see Fig. 16).

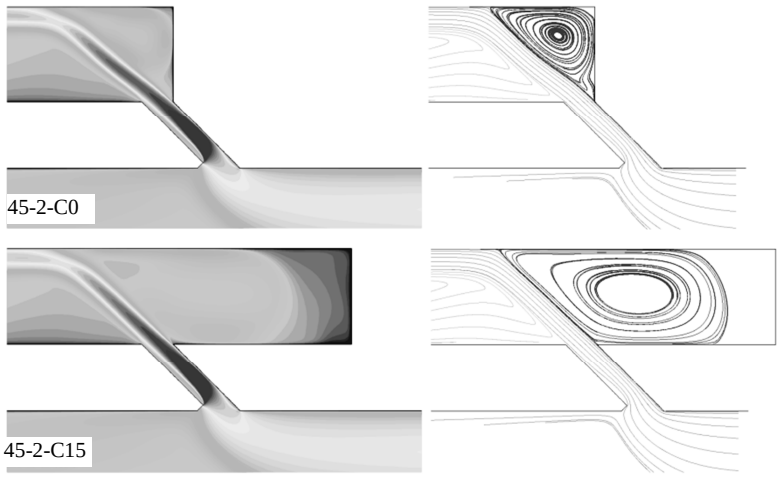

Fig. 16 Flow field in IRC inlet slot, variants 45-2

For other variants, C5 and C15, the character of the vortex forming is similar as it was described in the previous section. In 5 mm cavity (C5) the vortex is more intensive than in the case of 15 mm cavity depth (C15). On the left side of the inlet slot skewed at 45°, regardless of the bevel edge, a small flow separation occurs. This one influences only a small area and the flow attaches to the wall again approximately at a half of the inlet slot height. The overall results are comparable to the results of the 90-2BE variant, but the difference between particular cavity depths is not as noticeable as it was in case of the vertical inlet slot.

4.4 Comparison of Experiment and Simulation Results

Figs 17 and 18 show a comparison of the experiment and the simulation results for the vertical inlet slot variants 90-2SE and 90-2BE. The C0 variant gives the best results for both the experiment and the simulation. The remaining C5, C10 and C15 variants give approximately the same results in the experiment, however in the simulation the C5 variant turned out to be worse than C10 and C15.

On the contrary, for the bevel edge variant (90-2BE) the numerical simulation gives better results than the experiment. In both cases, for the C0 variants there is a significant shift towards higher air mass flow rates and higher σ_{IRC} coefficients compared to C5 and C15 variants. The numerical simulation again evaluated the C5 variant as the worst, although the difference between C5 and C15 variants are not significant.

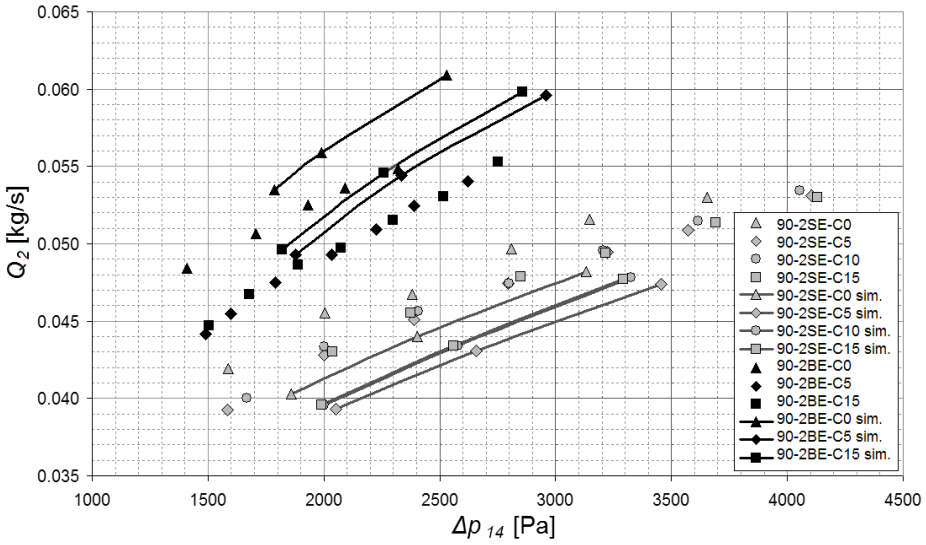

Fig. 17 Experiment and simulation results comparison

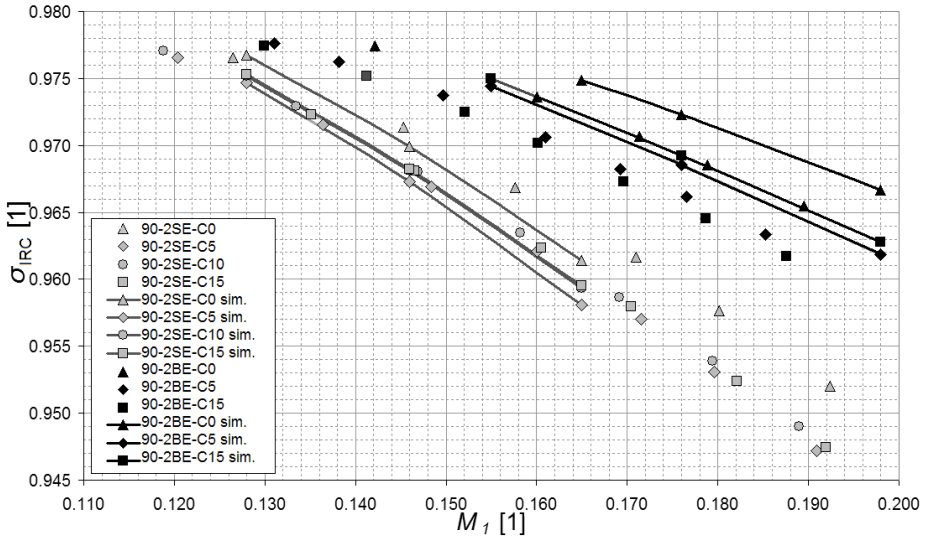

Fig. 18 Experiment and simulation results comparison

Some discrepancy between the experiment and the simulation in Fig. 17 and Fig. 18 may be caused by numerous factors, e.g. an uncertainty of the measured parameters and inaccurate model geometry on the one hand and a definition of proper turbulence model and simplified boundary conditions on the other hand. However, essential is the fact that the influence of particular modifications to the inlet slot keeps the same character in both the experiment and the simulation.

5. Conclusion

The experiment and the simulation have clearly shown that the most significant pressure losses in the recirculation channel are generated in the inlet slot. The inlet slot width and its edge modification have a fundamental influence on the IRC airflow. The inlet slot of 2 mm width caused relatively large pressure losses. After increasing its width just by 0.5 mm the pressure losses significantly decreased. The sharp edge of the inlet slot caused large pressure losses as well, while the edge bevelled just by $0.5 \times 45°$ performed much better.

The examined influence of the inlet slot angle showed that the effect of the inlet slot angle is connected to the cavity depth. In terms of low pressure losses and high IRC air mass flow rate, the variant 90-2.5BE-C0 (2.5 mm vertical inlet slot with bevel edges and no cavity) can be considered as the most suitable variant. The skewed variants 45-2.5-C15 and 60-2.5- C15 both reached slightly worse results, but still good enough. This documents the fact that both vertical and skewed inlet slots are used by manufacturers in practice.

Recommendations for IRC design:

- Inlet slot should always have bevel edges.
- Inlet slot width should be greater than 2 mm.
- The lowest pressure losses are reached by a vertical inlet slot with no cavity.
- It is possible to use a skewed inlet slot. In this case, attention must be paid to the sharp edge of the inlet slot which should be sufficiently rounded or beveled to prevent the flow separation. In case of the skewed inlet slot the IRC should be manufactured with a cavity on its end.

The IRC design is closely connected with the complex design of a centrifugal compressor, as the pressure distribution along the compressor casing significantly influences the pressure gradient on the IRC, which is fundamental for its function. Therefore, this article presents only some general recommendations for IRC design. Its particular form and position in the compressor casing must be designed together with the compressor itself.

Acknowledgement

This research work represents a part of the Specific Research Project of the Department of Aircraft and Rocket Technologies at University of Defence, Brno.

References

[1] KMOCH, P. *Theory of Aircraft Engines, Part I* (in Czech). Brno: Military Academy. 2002.

[2] KMOCH, P. and JÍLEK, A. Extension of High Pressure Centrifugal Compressor Steady Operation. In *KOKA 2006 – Almanac of Abstracts.* Praha: ČZU v Praze, 2006, p. 32.

[3] HUNZIKER, R., DICKMANN, HP. and ERICH, R. Numerical and Experimental Investigation of a Centrifugal Compressor Within an Inducer Casing Bleed System. In *4th European Conference on Turbomachinery – Conference Proceedings*. Padova: SGE, 2001. Also *Proceedings of the Institution of Mechanical Engineers Part A Journal of Power and Energy*, 2001, vol. 215, no. 6, p. 783-791. DOI: 10.1243/0957650011538910.

[4] YMAGUCHI, S., YMAGUCHI, H., GOTO, S., NAKAO, H. and NAKANUTA, F. The Development of Effective Casing Treatment for Turbocharger Compressors. In *Proceedings of 7th International Conference on Turbochargers and Turbocharging*. IMechE C602/008/2002, 2002, p. 23-32.

[5] BABÁK, M. CFD Analysis of a Surge Suppression Device for High Pressure Ratio Centrifugal Compressor. In *ANSYS Conference*. Frymburk: SVS FEM, 2010.

[6] SIVAGNANASUNDARAM, S., SPENCE, S., EARLY, J. and NIKPOUR, B. Experimental and numerical analysis of a classical bleed slot system for a turbocharger compressor. In *10th International Conference on Turbochargers and Turbocharging*, London: Woodhead Publishing, 2012.

[7] SIVAGNANASUNDARAM, S., SPENCE, S., EARLY, J. and NIKPOUR, B. An Investigation of Compressor Map Width Enhancement and the Inducer Flow Field Using Various Configurations of Shroud Bleed Slot. In *ASME Turbo Expo 2010*. Glasgow: ASME, 2010.

[8] SIVAGNANASUNDARAM, S., SPENCE, S., EARLY, J. and NIKPOUR, B. Map Width Enhancement Technique for a Turbocharger Compressor. In *ASME Turbo Expo 2012*. Copenhagen: ASME, 2012.

[9] PARK, C.-Y., CHOI, Y.-S., LEE, K.-Y. and YOON, J.-Y. Numerical Study on the Range Enhancement of a Centrifugal Compressor with a Ring Groove System. *Journal of Mechanical Science and Technology,* 2012, vol. 26, no. 5, p. 1371-1378. DOI 10.1007/s12206-012-0320-z.

[10] JÍLEK, A. *Airflow at Centrifugal Compressor Inlet.* (in Czech) [Ph.D. Thesis]. Brno: University of Defence, 2008.

[11] POLEDNO, M. *Enhancement of Stable Operating Region of Centrifugal Compressors* (in Czech) [Ph.D. Thesis]. Brno: University of Defence, 2014.

[12] ČSN EN ISO 5167-1 *Measurement of liquid flow by means of pressure differential devices inserted in circular cross-section conduits running full – Part 1: General principles and requirements* (in Czech). Praha: ČNI, 2003.